X-ray study of bilayered tilted structures in liquid crystalline side chain methacrylic polymers

EDUARDO A. SOTO-BUSTAMANTE*, RAFAEL VERGARA-TOLOZA, DANILO SALDAÑO-HURTADO and PATRICIO NAVARRETE-ENCINA

Universidad de Chile, Facultad de Ciencias Químicas y Farmacéuticas, Casilla 233, Santiago 1, Chile

The synthesis and measurement of thermodynamic properties of six methacrylate-based polymers were undertaken to observe the relationship between structural aliphatic features and mesophase properties. X-ray measurements on some of the polymers investigated show, as expected, the existence of bilayered smectic phases SmC_2 and SmA_d. Taking into account our previous results, an interesting trend in the tilt angle was found that might be related to the difference in alkyl chain substitution.

1. Introduction

Side chain liquid crystal polymers continue to attract attention, and a significant amount of research is devoted to their properties, not only because of their considerable application potential in a wide range of advanced electro-optic technologies [1] but also because they provide a quite demanding challenge to our understanding of self-assembly in condensed matter [2]. A side chain liquid crystal polymer normally consists of three components: a polymer backbone, a flexible spacer and an aromatic core. Changing the structure of some of these components may modify the properties of such polymers. Thus, by varying the length of the aliphatic part of the mesogenic group, it is possible to gain some control over transition temperatures; to a lesser extent, the exhibited phase sequences may also be modified [3].

In previous work, the observation of ferro- and antiferro-electricity in liquid crystalline materials was to a great extent correlated with the presence of at least one chiral centre in the molecule. Unexpectedly we found an interesting achiral system with unusual electrical properties unknown in such systems. Our samples consisted of mixtures of side chain liquid crystalline polymers with their respective monomers [4].

If our focus is to design new materials having targeted properties, in a rational manner, we must first establish and understand the relationships between structure and properties of these mixtures. As part of a continuing research programme probing the fundamental structure–properties relationship in side chain liquid crystal polymers [5–9], we firstly reported the X-ray structure determination in some side chain polymers [7, 9] and the phase sequence of monomers [10]. Now we report the X-ray structure characterization of six new methacrylate side chain polymers.

In accordance with our previous work, the same acronym is used: PM*n*R*m* where P denotes the backbone polymer; M*n* is a methacrylate group with *n* methylene units as aliphatic spacer; R*m* is a rigid resorcylphenylimine core group (*R*) possessing an alkoxy flying tail with *m* methylene units located in the *para*-position and bonded to M*n*. In figure 1 the general structure of the polymers is displayed.

*Author for correspondence; e-mail: esoto@ciq.uchile.cl

2. Experimental

The compounds were synthesized using the convergent synthetic pathway described in previous communications [11, 12]. A minimal variation in the purification step of the polymer was carried out using Soxhlet extraction with methanol, instead of repeated precipitation of the swelled polymer with methanol from concentrated toluene solution. The characterization was done by ^{1}H NMR spectroscopy using a 300 MHz spectrometer (Bruker, WM 300), infrared spectroscopy (FTIR Paragon Spectrometer, 100PC) and elemental analysis (Perkin Elmer, 240 B). For the sake of clarity the analytical data for poly-{2-methyl-2-propenoic acid 4-[3-hydroxy-4-(6-undecyloxyphenylimino)methylphenoxy]hexyl ester} (PM6R11) are presented. ^{1}H NMR, δ ppm, $CDCl_3$: 13.78 (s, 1H, Ph−O**H**); 8.27 (s, 1H, Ph−C**H**=N); 7.05 (m, 3H, Ph−**H**); 6.75 (m, 2H, Ph−**H**); 6.35 (m, 2H, Ph−**H**); 3.78 (m, 6H, **CH$_2$**−OPh, **CH$_2$**−O$_2$C); 1.70–1.15 (m, 26H, −CH$_2$−**CH$_2$**−**CH$_2$**−CH$_2$−; C**H$_3$**−C−C$_3$); 0.80 (t, 3H, −CH$_2$−C**H$_3$**). IR (KBr) cm^{-1}: 1720 s (ν C=O),

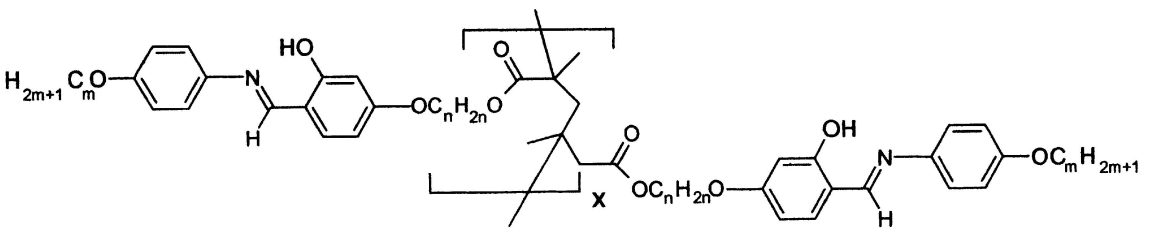

Figure 1. Investigated side chain polymers: $n = 4$, $m = 5$–6, 8; $n = 6$, $m = 7$, 9, 11.

1615 s (ν C=N), 1288 s, 1248 s, 1193 s, 1172 w, 1137 m, 1115 m (ν C–O), 645 m, 588 m, 532 s, 467 m. $(C_{34}H_{49}NO_5)_n$ $(M = 551.76)_n$: calc. C 74.00, H 8.97, N 2.54; found C 74.30, H 9.08, N 2.75%.

The molecular mass $\bar{M}_w$ and the polydispersity index *DI* for the polymers were determined by gel permeation chromatography (GPC) using a Waters 600 Controller microflow pump, with a Waters 410 Differential Refractometer as detector. The standard for calibration was polymethylmethacrylate (PMMA) and a styragel HT4 (Waters) column, using tetrahydrofuran HPLC grade as eluent with a flow rate of 0.3 ml min^{-1}.

The phase transition temperatures were determined using a differential scanning calorimeter (Mettler Toledo FP84HT, FP 90 temperature processor), accuracy ± 0.1 K. The temperature-dependent investigations of liquid crystal textures were carried out in a polarizing microscope (Leica, DMLP), equipped with a heating stage (HS-1, Instec). A video camera (Panasonic WVCP414P) installed on the polarizing microscope, is coupled to a video capture card (Miro DC-30) that allows real-time video capture and the saving of sequential image frames from these videos to a personal computer. The samples were supported between glass plates.

X-ray measurements were carried out using CuK_α radiation. The samples were contained in 1.0 mm glass capillaries (Lindemann) and held in a copper block. Data for aligned samples in the small angle region were obtained using a focusing horizontal two-circle X-ray diffractometer (STOE, STADI 2) with a linear position-sensitive detector [13, 14]. The temperature was stabilized within the range 30 to 250°C $\pm$ 0.5°C during the measurements.

3. Results

3.1. *Thermodynamic properties*

The phase transition temperatures and molecular mass characterization for polymers not reported here, but included in the following discussion, have been described in previous communications [7, 9, 12]. For the sake of clarity they will be denoted with a superscript alluding to the reference. In case of PM6R6 the reported molecular mass corresponds to a freshly polymerized sample. The transition temperatures were confirmed by DSC and polarizing microscopy; results are summarized in table 1.

3.2. *X-ray investigations*

X-ray studies were carried out on six compounds: PM4R5, PM4R6, PM4R8, PM6R7, PM6R9 and PM6R11. All sample diffractograms below the isotropic transition point show sharp small angle peaks associated with the smectic character of the mesophases, and diffuse wide angle peaks related to the degree of disorder within the smectic layers, showing liquid-like in-plane order (see figure 2).

The molecular length *L* of the corresponding monomers, calculated using MOPAC93 molecular approximation software, for each of the polymers studied by XRD are given in table 2. *L* equals the distance on the molecule,

Table 1. Phase transition temperature and enthalpy change on heating for the investigated samples, as well as average molecular mass $\bar{M}_w$, polydispersity index *DI* and degree of polymerization P_w for the LC polymers.

Sample	Mesophase	Enthalpy J g^{-1}	$\bar{M}_w$/g mol^{-1}	*DI*	P_w
PM4R5	g–50.8–SmC_2–187.1–I	21.97	124,813	1.703	284
PM4R6	g–58.7–SmC_2–191.3–I	13.80	86,229	1.786	190
PM4R8	g–57.8–SmC_2–201.3–I	15.62	129,607	1.193	269
PM6R6[7]	g–82.0–SmC_2–157.0–SmA_d–173.0–I	10.30–4.32	77,575	1.756	161
PM6R7	g–83.4–SmC_2–162.7–SmA_d–176.7–I	7.78–2.70	55,126	1.313	111
PM6R8[12]	g–82.0–SmC_2–180.0–I	16.40	81,500	2.100	160
PM6R9	g–62.2–SmC_2–183.6–I	18.55	115,209	1.313	220
PM6R10[9]	g–64.2–SmC_2–190.3–I	19.02	104,300	2.370	194
PM6R11	g–70.6–SmC_2–195.3–I	19.45	102,016	1.587	185
PM6R12[9]	g–nj.d.–SmC_2–190.5–I	21.20	108,100	2.609	191

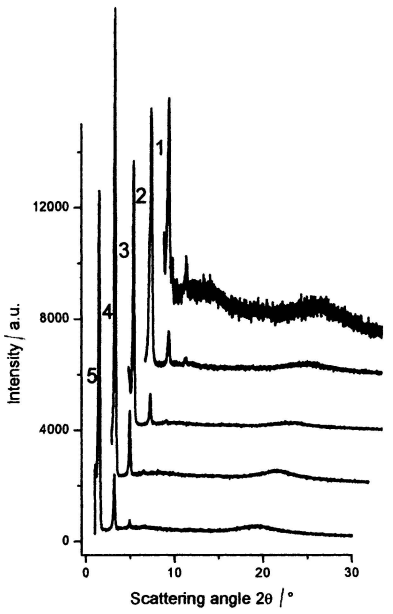

Figure 2. X-ray diffraction pattern for: (1) PM4R5 at 190°C, (2) PM4R6 at 160°C, (3) PM4R8 at 120°C, (4) PM6R9 at 125°C and (5) PM6R11 at 170°C.

Table 2. Calculated length of molecules L, average molecular distance in the layers D, experimental interlayer distance d, calculated ratio $d/2L$ and tilt angle β in the smectic C phase at the indicated temperature.

Sample	L/Å	D/Å	d/Å	$d/2L$	β/°	Temp./°C
PM4R5	26.30	4.67	47.88	0.91	24.50	120.0
PM4R6	28.19	4.54	52.16	0.93	21.56	120.0
PM4R8	30.41	4.52	53.91	0.89	27.58	120.0
PM6R6[7]	30.88	4.61	49.90	0.81	36.10	80.0
PM6R7	32.18	4.32	50.44	0.78	38.40	80.0
PM6R8[7]	33.42	4.39	50.86	0.76	40.45	80.0
PM6R9	34.72	4.59	57.94	0.84	33.45	85.0
PM6R10[9]	35.96	4.63	60.09	0.84	33.45	89.7
PM6R11	37.26	4.50	61.32	0.82	34.63	80.0
PM6R12[9]	38.53	4.59	63.67	0.83	34.29	89.7

in the stretched conformation, between the last carbon atom in the aliphatic flying tail and the first methylenic carbon atom of the methacrylic group. Taking the experimental interlayer distance d and twice the molecular full-length ($2L$ values in table 2), we can calculate the tilt angle β ($\beta = \arccos d/2L$). In this table the average molecular distance in the layers D, experimental interlayer distance d and tilt angle β of the mesophases at the indicated temperature are also included.

The experimental interlayer distance, taken from X-ray measurements, is shown in figure 3 (*a*) for the M4 Series and in figure 3 (*b*) for the M6 Series. The temperature variation of the first order reflex shows for PM6R7, the

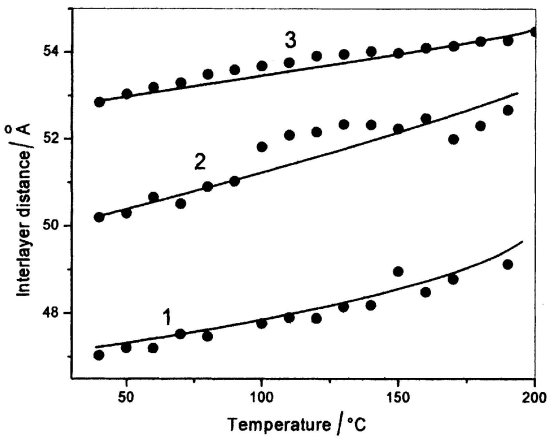

a)

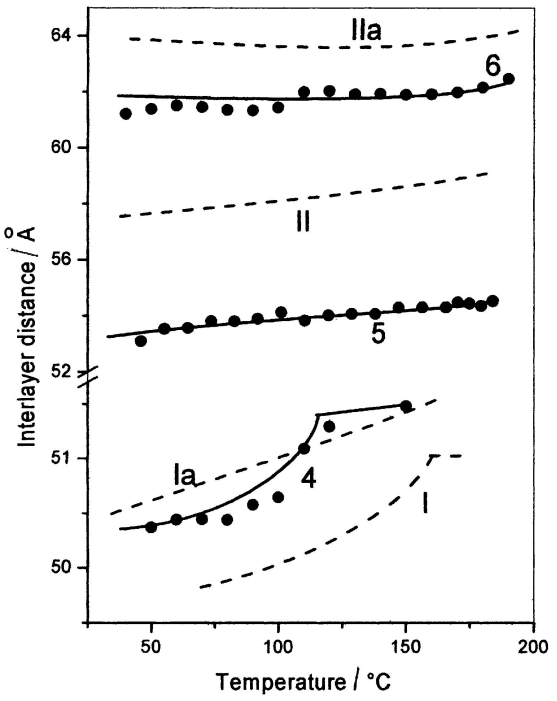

b)

Figure 3. Temperature dependence of the interlayer distance on cooling: (*a*) M4 series (1) PM4R5, (2) PM4R6, (3) PM4R8; (*b*) M6 series (4) PM6R7, (5) PM6R9, (6) PM6R11. Dashed lines: (I) PM6R6 and (Ia) PM6R8 from ref. [7]; (II) PM6R10 and (II) PM6R12 from ref. [9].

existence of two different mesophase regions, smectic A_d and smectic C_2, figure 3 (*b*) curve 4. The other mixtures show a rather monotonic behaviour that corresponds to a smectic C_2 phase. The observed SmA_d to SmC_2 change correlates reasonably well with the transition temperatures obtained by DSC.

As can be seen from table 2, where previous results [7, 9] are included, M6 is the most widely studied series, the following discussion will be focused mainly on this series.

4. Discussion

Table 1 summarizes the molecular mass characterization of the samples studied. No traces of monomer or oligomer fractions in the samples were detected in the chromatograms. This fact, together with a quite low dispersion index *DI* ranging from 1.2 to 1.8, reflects the polymeric nature of the freshly polymerized samples. If we compare these values with those previously reported for PM6R8, PM6R10 and PM6R12 [7, 9], between 2.1 and 2.6, it is clear that the soxhlet purification process with methanol is far more efficient than repeated precipitation with the same solvent, for obtaining samples with a good *DI* range from the crude polymers.

As has already been described [10], the monomers show the simultaneous occurrence of monolayering smectic A and C phases. Even in the case of M4R4 and M4R5 an I–N–A–C phase sequence is observed, with the presence of a narrow nematic phase near the isotropic state. For polymers the situation is different, where the occurrence of bilayering smectic phases were reported. For PM6R8, PM6R10 and PM6R12 [7, 9], we reported the existence of a SmC_2 phase in a broad temperature range. In an early report [7] we also describe the situation of PM6R6 which shows the simultaneous presence of a SmA_d and SmC_2 phases.

In this particular work, the PM4R5, PM4R6, PM4R8, PM6R7, PM6R9 and PM6R11 samples show a similar behaviour to the previously reported compounds, i.e. the interlayer periodicity significantly exceeds the length L of the side chains. This can be demonstrated by the ratio $d/2L = 0.75$–0.91 depending on temperature and polymer (see table 2). This implies the existence of a bilayered arrangement of side chain mesogenic units in smectic planes, as expected. Therefore we assume bilayered structures in which side chains are tilted with respect to the normal to the layer. In another structural model the mesogenic side chains, being orthogonal to the smectic planes, partially overlap each other, giving a SmA_d structure.

To clarify this situation, the experimental interlaying distance d versus temperature was estimated for each case. PM6R7 displays the same break in d-values as PM6R6 [7], which is related to the SmA_d–SmC_2 phase transition, see figure 3(*b*), curve 4. This situation is characteristic of phase transitions between orthogonal and tilted smectic phases. On the other hand in the SmC_2 phase of polymers PM6R9 and PM6R11 the layer spacing d slightly decreases with decreasing temperature. This behaviour is typical of strong first order transitions from the isotropic to tilted phases associated with a large jump in tilt angle values at the phase transition point.

A most interesting trend of d-values against temperature is observed when considering the whole M6 series. In figure 3(*b*) the dashed lines represent the d-value trends for previously investigated samples [7, 9]. Curve I represents PM6R6 and curve Ia represents PM6R8 from reference [7], while curves II and IIa represent PM6R10 and PM6R12, respectively [9]. Regarding the d-values in table 2, it is possible to see a characteristic relationship between experimental thickness layering d and the number of methylenic groups in the aliphatic chain. The shorter side chain polymers (PM6R6 to PM6R8) are compressed at around the same interlayer distance, whereas the longer side chain polymers (PM6R9 to PM6R12) are almost equally distributed in ascendant order with respect to d. Figure 4 was prepared to show the variation of the interlayer distance d and the tilt angle β (at a constant temperature of 80°C, where all samples exist in the SmC_2 phase) with the number of methylenic units m in the mesogenic groups. At the left side and in filled circles, the dependance of the interlayer distance shows two well defined tendencies. For compounds having low values of m (PM6R6 to PM6R8), no alkyl substitution dependance is observed; but the dependance becomes significant for higher values of m (PM6R9 to PM6R12). The opposite behaviour is observed for the tilt angle for the SmC_2 phase (values at the right axis of the graph and represented by open circles).

These tendencies may be explained if we consider the tilt angle dependance of the SmC_2 phases, related to the increase in molecular length. Beyond an angle of 45°, no further increase is observed and, the next polymer in the series again adopts an adequate inclination of the tilt angle value of around 33° to 34°. This effect was not observed in the corresponding monomers in the series [10]. Polymers possess double layered smectic phases and therefore the aliphatic character due to the alkyl chain is twice as important for these materials. Then, over a certain aliphatic to aromatic ratio, the system begins to

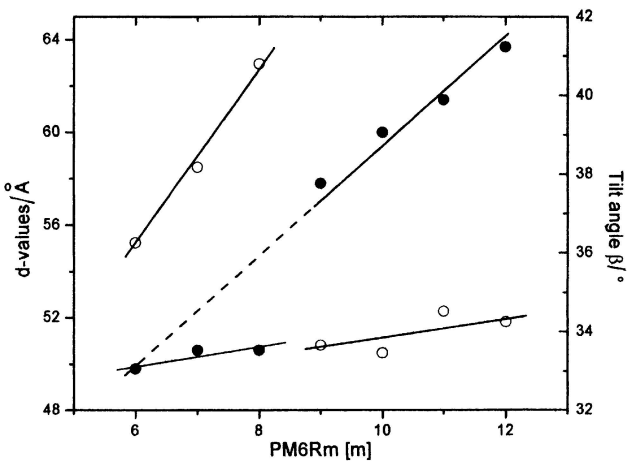

Figure 4. Dependence of the interlayer distance d (filled circles) and tilt angle β (open circles) of the smectic C2 phase at 80°C on mesogenic group length.

stabilize in such a way as to increase the interlayer distance instead of the tilt angle. Therefore the tilt angle does not 'saturate' at 45°; it decreases to 32° and then remains almost constant.

This gap in the tilt angle dependance on *m* is clearly seen in figure 4. In this second situation, it seems likely that the system requires a higher rigidity to allow a second dependance of the tilt angle of the SmC_2 phase on increasing molecular length. The ratio of aliphatic to aromatic tails does not permit a secondary angular dependance, which becomes evident beginning with PM6R9. Therefore as the *m* value increases, the interlayer distance *d* does also.

5. Conclusions

The new compounds with higher side chains PM6R9 and PM6R11 are ordered in a smectic C_2 phase over the whole temperature range investigated, whereas for compound PM6R7, on cooling, the phase sequence smectic A_d–before the isotropic state–and smectic C_2 phase–before the glassy state–could be rationalized.

As soon as the length of the spacer chain length increases, and as *m* increases, the interlayer distance also increases, but an upper limit of about 45° in the tilt angle cannot be surpassed. The gap between shorter and longer spacer chain length compounds is produced by the angular dependance of the tilt angle with *d*.

There seems to exist a relationship between the predominance of aliphatic or aromatic character in the side chain mesogens, since two tendencies have been clearly observed. On the one hand, for the aromatic predominant mesogens, a tilt angle dependance is observed. On the other hand the aliphatic predominant mesogens present a strong interlayer distance dependance, figure 4 (*b*).

With reference to our previous results, when comparing monomers and polymers an obvious difference in the interlayer distance *d* of the mesophases can be seen. A monomer presents mono-layered structured mesophases, while a polymer shows bi-layered mesophases.

E.A.S.B is grateful for financial support from Projects FONDECYT 2000 Nr. 1000845, 7000845 and Volkswagen Stiftung, project I/77005. We also thank Prof. W. Haase for helpful and stimulating discussion.

References

[1] Blackwood, K. M., 1996, *Science*, **909,** 273.
[2] Imrie, C. T., 1996, *Polymeric Material Encyclopedia*, Vol. 5, edited by J. C. Salamone (Florida: CRC Press), p. 3770.
[3] Cook, A. G., and Imrie, C. T., 1999, *Mol. Cryst. liq. Cryst. Sec. A*, 2699.
[4] Soto Bustamante, E. A., Yablonsky, S. V., Beresnev, L. A., Blinov, L. M., Haase, W., Dultz, W., and Galyametdinov, Yu. G., 1995, DE 195 47 934; 1997, EP 780 914, 1997 JP 237 921/907, 1997, US 5 833 833.
[5] Soto Bustamante, E. A., Yablonskii, S. V., Ostrovskii, B. I., Beresnev, L. A., Blinov, L. M., and Haase, W., 1996, *Chem. Phys. Lett*., **260,** 447.
[6] Soto Bustamante, E. A., Yablonsky, S. V., Ostrovskii, B. I., Beresnev, L. A., Blinov, L. M., and Haase, W., 1996, *Liq. Cryst*., **21,** 829.
[7] Ostrovskii, B. I., Soto Bustamante, E. A., Sulianov, S. N., Galyametdinov, Yu., and Haase, W., 1996, *Mol. Mat*., **6,** 171.
[8] Soto Bustamante, E. A., Navarrete Encina, P. A., Weyrauch, T., and Werner, R., 2000, *Ferroelectrics*, **243,** 125.
[9] Werner, R., Soto Bustamante, E. A., Navarrete Encina, P. A., and Haase, W., 2002, *Liq. Cryst*., **29,** 713.
[10] Soto Bustamante, E. A., Saldaño, D., Vegara-Toloza, R., Navarrete Encina, P. A., Athanasopuolous, M. A., and Haase, W., 2003, *Liq. Cryst*. **30,** 17.
[11] Soto Bustamante, E. A., and Haase, W., 1997, *Liq. Cryst*., **23,** 603.
[12] Soto Bustamante, E. A., Galyametdinov, Yu. G., Griesar, K., Schuhmacher, E., and Haase, W., 1998, *Macromol. Chem. Phys*., **199,** 1337.
[13] Klämke, W., Fan, Z. X., Haase, W., Müller, H. J., and Gallardo, H. D., 1989, *Ber. Bunsenges. Phys. Chem*., **93,** 478.
[14] Fan, Z. X., and Haase, W., 1991, *J. chem. Phys*., **95,** 6066.